06

# The possibility of practical application of citrogypsum in engineering

© T.B. Nikulicheva,[1] V.S. Zakhvalinskii,[1] E.A. Pilyuk,[1] I.S. Nikulin,[1] V.V. Vyazmin,[1] M.V. Mishunin,[1] M.Yu. Saenko,[1] O.A. Telpova,[1] N.I. Alfimova,[2] T.A. Erina[1]

[1]Belgorod National Research University,
308015 Belgorod, Russia
[2]Belgorod State Technological University named after V.G. Shukhov,
308012 Belgorod, Russia
e-mail: zakhvalinskii@bsu.edu.ru, t_nikulicheva@inbox.ru

*Received May 5, 2023*
*Revised July 17, 2023*
*Accepted July 19, 2023*

At present, the problem of using as functional materials such materials that are a by-product of technological processes and accumulate in the form of production waste is becoming more relevant. We have studied two groups of samples. The first group became the basis for a new material for the air humidity sensor, which was obtained from the waste products of citric acid production. Samples of citrogypsum (calcium sulfate dihydrate, i.e. $CaSO_4 \cdot 2H_2O$) doped with copper sulfate ($CuSO_4 \cdot 5H_2O$) were prepared. The dependence of the impedance on the relative humidity of samples of three thicknesses was carried out. The frequency dependences of complex resistance and relative permittivity on relative humidity are measured. The second group of samples obtained from citrogypsum was a powder consisting of $CaSO_4 \cdot 2H_2O$ whiskers. Whiskers $CaSO_4 \cdot 2H_2O$ were used to create composites based on epoxy resin. An improvement in the properties of the composite was recorded in the study of tensile and compressive stresses of the samples. This article shows the possibility of practical application of $(CaSO_4 \cdot 2H_2O)_{0.95} - (CuSO_4 \cdot 5H_2O)_{0.05}$ — as a new air humidity sensor material and improvement of the mechanical properties of the composite based on epoxy resin and $CaSO_4 \cdot 2H_2O$ whiskers.

**Keywords:** composite, citrogypsum, resistive humidity sensor, impedance spectroscopy, whiskers.

DOI: 10.61011/TP.2023.09.57362.113-23

## Introduction

In the last decades, intelligent electronic systems are rapidly developing, they largely improve technological processes in industry and agriculture, the quality of life and health of people. However, the processes of obtaining the materials from which electronic devices are made are a source of increasing waste, putting a strain on the environment and posing a threat to human health [1,2]. The approach to a partial solution of these problems, consisting in the use of environmentally friendly and common in nature materials, especially if these materials are wastes of technological processes and are utilized in the production of electronic components, seems relevant to us.

The present work is devoted to the use of citrogypsum ($CaSO_4 \cdot 2H_2O$), which is a waste product of the technological process of food citric acid production, as a material for the manufacture of air humidity sensors and as a reinforcing filler material in an epoxy matrix, which requires modification of its physical properties.

A wide range of materials [3–6] are used to make air humidity sensors, and the sensors differ in physical principles of operation and construction [7–9]. The use of new materials, including wastes of technological production, especially environmentally friendly ones, will reduce the ecological load on the environment and make it cheaper to manufacture sensors while maintaining their functional characteristics. Humidity sensors are used in home comfort [10], agriculture [11], medicine [12], food industry [13]. Regardless of the material from which the sensors are made, they must respond to humidity by changing at least one of the parameters such as resistance, capacitance, pH, and color of the material. In addition, the humidity sensor must either continuously record the measured parameter as the relative humidity increases and decreases, or be able to repeatedly and quickly return to its initial state prior to measurement. Natural materials or waste materials from industrial processes need additional purification or modification to be used as a sensor material.

Another attractive area of application of industrial waste is its use after special treatment as a reinforcing filler in composite polymer materials. The use of epoxy matrix composites is increasing due to their availability, low cost, and properties that meet the requirements of aerospace, automotive, and other industrial applications [14]. Such application of wastes from technological processes is beneficial from the point of view of increasing reliability and durability of materials with epoxy matrix and reducing the technogenic impact on the environment. The utilization of mechanical properties requires more attention to the study of the deformation phenomenon of composites [15].

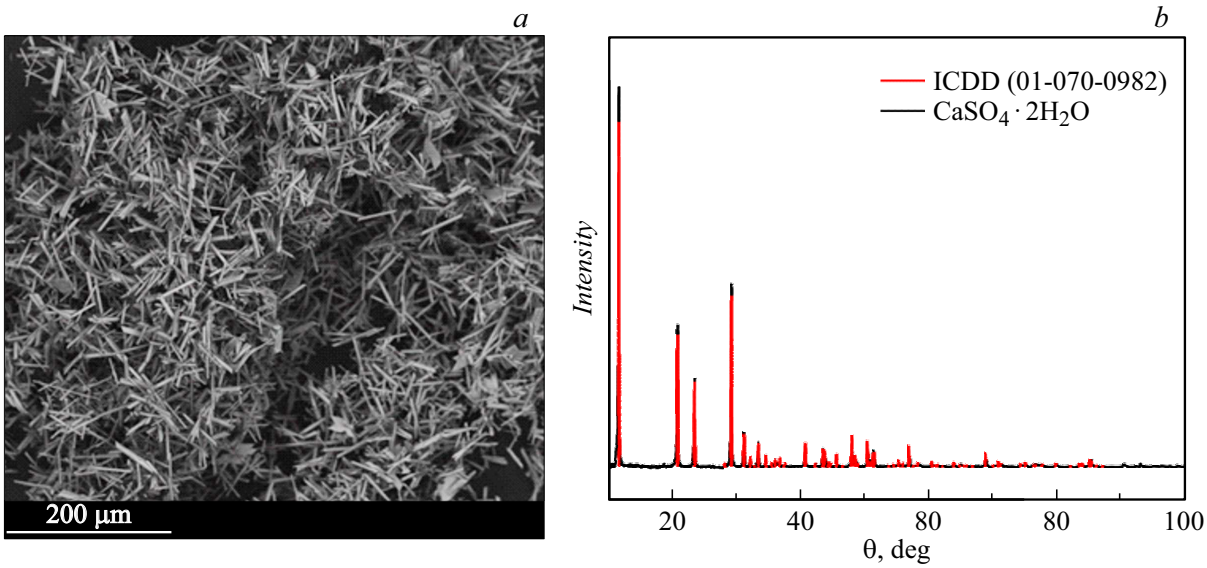


**Figure 1.** SEM micrograph of $CaSO_4{\cdot}2H_2O$ whiskers obtained on FEI Quanta 600 FEG ($a$), X-ray spectrum of $CaSO_4{\cdot}2H_2O$ whiskers and test spectrum from ICDD (01-070-0982) database obtained on Rigaku SmartLab diffractometer ($b$).

## 1. Materials and methods

### 1.1. Composite samples: $(CaSO_4{\cdot}2H_2O)_{0.95}-(CuSO_4{\cdot}5H_2O)_{0.05}$

Citrogyps, which is a waste product of biochemical production of citric acid [16,17] (Belgorod, Russia), served as a source material for the manufacture of air humidity sensors. The physical and chemical properties of citrogypsum are described in [18]. Citrogyps (calcium sulfate dihydrate, i.e. $CaSO_4{\cdot}2H_2O$)for 1 h at 200 °C was dehydrated and anhydrite ($CaSO_4$) was obtained in the first step. Then, anhydrite soaking in atmospheric air for 24 h yielded citrohypsum semihydrate($CaSO_4{\cdot}0.5H_2O$). Next, composite samples $CaSO_4{\cdot}2H_2O)_{0.95}-(CuSO_4{\cdot}5H_2O)_{0.05}$ were obtained from citrogypsum semihydrate. Copper sulfate ($CuSO_4{\cdot}5H_2O$) was used to modify the properties of citrogypsum. Stoichiometric suspensions were prepared from ($CaSO_4{\cdot}0.5H_2O$) and ($CuSO_4{\cdot}5H_2O$) on analytical scales LV 210-A with an accuracy of 0.0001 g. Copper sulfate was dissolved in water and citrogyps was added to the resulting solution, which was reduced by interaction with water to calcium sulfate dihydrate. The resulting wet mass of material was pressed at a pressure of 22 MPa. After air-drying at room temperature for 2 h, the samples were cut into a parallelepiped shape with a contact surface area of 9.2×7.2 mm and thicknesses of 1.1, 2.2, and 4.4 mm. The energy-dispersive X-ray spectrum (EDX) of the slurry and the surface morphology of the sample were examined on a Quanta 600 FEG scanning election microscope. Electrical contacts are made by applying silver to the contact surface by HF-magnetron sputtering on the VN-2000 unit. The use of HF-magnetron sputtering avoided overheating of the samples. Probes for studying electrophysical properties were attached to the sample with silver-containing adhesive.

The samples $(CaSO_4{\cdot}2H_2O)_{0.95}-(CuSO_4{\cdot}5H_2O)_{0.05}$ were a parallelepiped-shaped capacitor analog with a contact surface area of 9.2 ×7.2 mm and thicknesses of 1.1, 2.2 and 4.4 mm with top and bottom sputtered silver liners. The conductivity of the samples was investigated by impedance spectroscopy. To measure electrical conductivity, an RLC AM-3026 AKTACOM meter was used in the frequency range of 200 Hz−5 MHz with an AC signal amplitude of 1 V without constant polarization. Measurements were performed at a constant temperature of 28 °C and a relative humidity range of 30 to 90%. Humidity and temperature were monitored using the AOSONG DHT11 sensor.

### 1.2. Polymer composite samples: whiskers $CaSO_4{\cdot}2H_2O$ as reinforcing filler in epoxy matrix

$CaSO_4{\cdot}2H_2O$ whiskers were prepared from citrogypsum, a waste product of the biochemical production of citric acid, by a method similar to [19]. FEI Quanta 600 FEG scanning election microscope examination (Fig. 1, $a$) showed that whiskers of different sizes were obtained. Based on the constructed histograms, the mean length (Fig. 2, $a$) and mean width (Fig. 2, $b$) were estimated to be 23.2±0.3 $\mu$m and 1.9±0.1 $\mu$m, respectively.

Quality control of $CaSO_4{\cdot}2H_2O$ material was carried out by X-ray diffraction analysis on a Rigaku SmartLab diffractometer, CuK$\alpha$-radiation ($\lambda = 1.5406$ Å, $U = 50$ kV, $I = 60$ mA)at room temperature in the range of $2\theta = 10 - 100°$. X-ray diffraction analysis showed that the spectrum (Fig. 1, $b$) of the obtained $CaSO_4{\cdot}2H_2O$ whiskers matched the spectrum of $CaSO_4{\cdot}2H_2O$ from the ICDD (01-070-0982) database. $CaSO_4{\cdot}2H_2O$ whiskers were used as

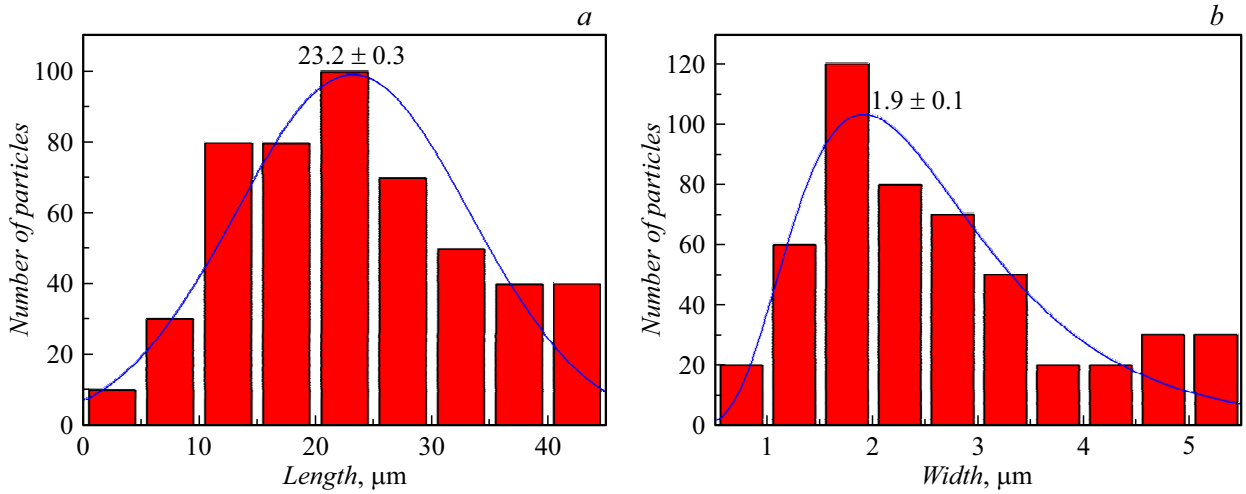


**Figure 2.** Histograms of particle (whiskers) size distribution obtained from SEM images: length ($a$) and width ($b$), respectively.

Energy-dispersive X-ray spectral (EDX) analysis of the sample $(CaSO_4 \cdot 2H_2O)_{0.95} - (CuSO_4 \cdot 5H_2O)_{0.05}$

| Element | O | Na | Si | S | Cl | Ca | Cu |
|---|---|---|---|---|---|---|---|
| Weight, % | 63.19 | 0.57 | 0.10 | 15.12 | 0.42 | 20.02 | 0.58 |
| At., % | 77.28 | 0.50 | 0.07 | 9.49 | 0.24 | 10.05 | 0.18 |

filler in ArtEpoxy epoxy resin. Whiskers were prewashed with alcohol and dried at 75 °C for 2 h. Composite samples containing 0, 5, 10, and 15% whiskers were poured into polyethylene molds and polymerized for 60 h at 50 °C. Tensile and compressive stresses were investigated on epoxy resin composite specimens with $CaSO_4 \cdot 2H_2O$ whisker filler prepared for measurements on an Instron 3369 universal testing machine. The tensile specimens were flat dumbbells and had a narrow part length $\sim$ 40 mm, width $\sim$ 5 mm and thickness $\sim$ 2 mm, respectively. The total length was 75 mm. The compression specimens were parallelepiped shaped and had length $\sim$ 6 mm, width $\sim$ 5 mm and thickness $\sim$ 3 mm, respectively. The strain rate was 0.1 mm/s.

## 2. Results and discussion

### 2.1. Composite samples $(CaSO_4 \cdot 2H_2O)_{0.95} - (CuSO_4 \cdot 5H_2O)_{0.05}$

Fig. 3, $a$ shows an image of the surface of the sample $(CaSO_4 \cdot 2H_2O)_{0.95}$–$(CuSO_4 \cdot 5H_2O)_{0.05}$, obtained with a Quanta 600 FEG scanning election microscope is presented. Fig. 3, $b$ shows the EDX spectrum obtained with a Quanta 600 FEG scanning election microscope. The table presents the results of the percentage and elemental compositions of the sample $(CaSO_4 \cdot 2H_2O)_{0.95}$–$(CuSO_4 \cdot 5H_2O)_{0.05}$.

The surface image (Fig. 3, $a$) shows dark granules of metallic copper. The composition of the obtained composite is confirmed by the data of EMF spectra (Fig. 3, $b$) and the table.

The method of experimental investigations consists in measuring in an alternating electric field the frequency dependences of the active ($R$), and reactive ($X$) components of the complex impedance: $Z = R + jX$, where $j$ — imaginary unit. The $(CaSO_4 \cdot 2H_2O)_{0.95} - (CuSO_4 \cdot 5H_2O)_{0.05}$ samples exhibit a controlled sensitivity of the total complex impedance $Z$ to humidity over a wide operating range from 40 to 80% relative humidity; the dependence is most pronounced at low frequencies (Fig. 4). Modification of citrogypsum with copper sulfate changed the properties of the obtained composite and increased its sensitivity to air humidity.

With increasing sample thickness from 1.1 to 2.2 and 4.4 mm, the value of the complex impedance $Z$ increased, e.g., at 40% RH (relative humidity) at 200 Hz from 50 to 100 MΩ, respectively. At frequencies above 100 kHz, the sensitivity to changes in relative humidity RH was minimal for all sample thicknesses. For all thicknesses, the complex resistance decreases sharply in the frequency range from 200 Hz to 1 kHz with increasing relative humidity. As the frequency increases from 200 Hz to 5 MHz, the impedance of an $Z$ sample with a thickness of 1.1 mm decreases, for example, from 50 M Ω to 2 kΩ at a relative humidity of 40%. At high frequencies from 100 kHz to 5 MHz, the value of $Z$ is small and varies slightly with increasing moisture content for all sample thicknesses and decreases with increasing frequency. Thus,

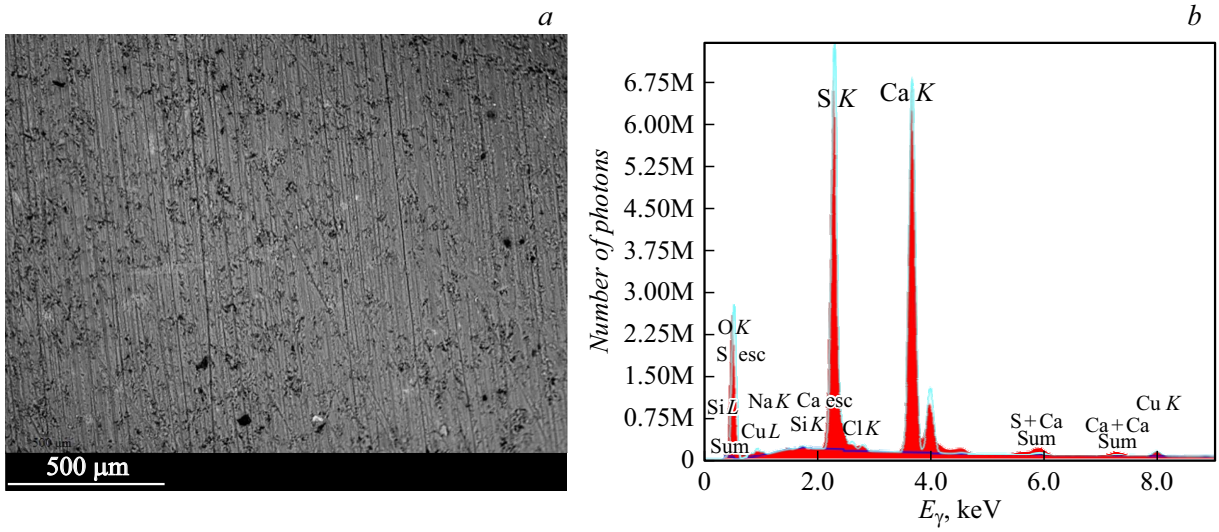


**Figure 3.** SEM micrograph of the sample $(CaSO_4 \cdot 2H_2O)_{0.95} - (CuSO_4 \cdot 5H_2O)_{0.05}$ slip surface using FEI Quanta 600 FEG, magnification ×150 (*a*); spectrum EDX of sample $(CaSO_4 \cdot 2H_2O)_{0.95} - (CuSO_4 \cdot 5H_2O)_{0.05}$ (*b*).

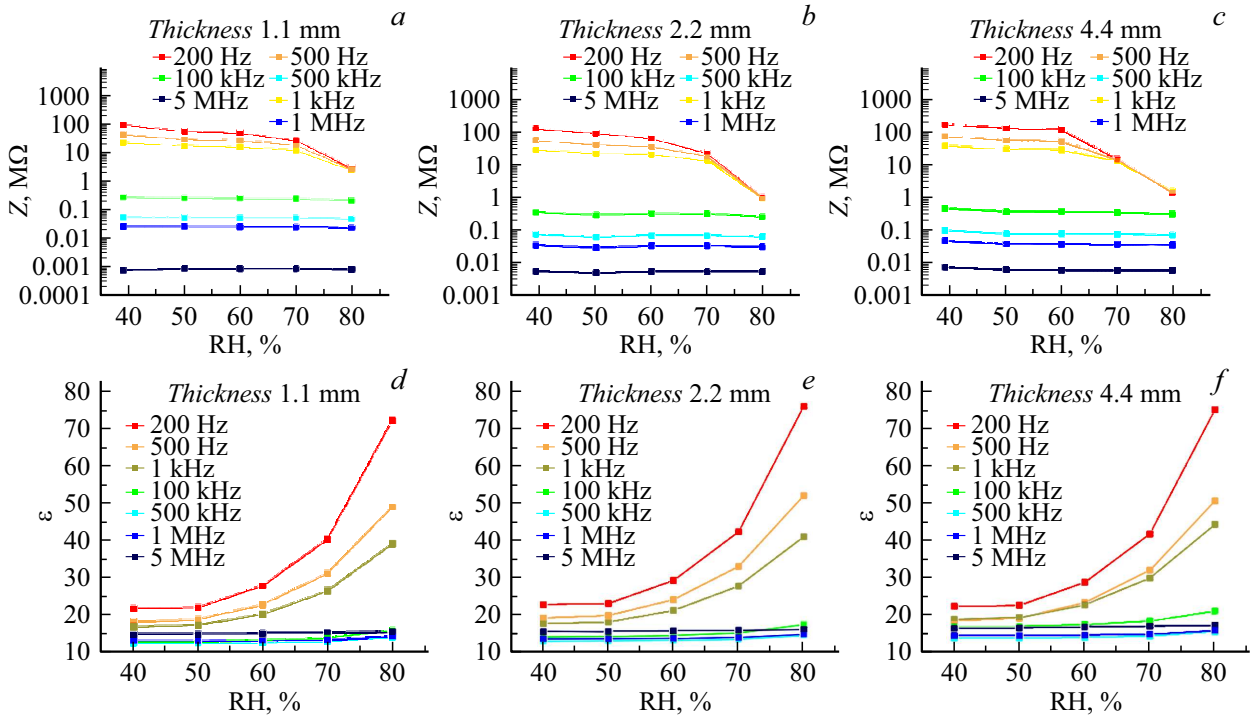


**Figure 4.** Dependence of complex resistance $Z$ on relative humidity of composite samples $(CaSO_4 \cdot 2H_2O)_{0.95} - (CuSO_4 \cdot 5H_2O)_{0.05}$ of three thicknesses — 1.1 (*a*), 2.2 (*b*), 4.4 mm (*c*). Dependence of dielectric constant $\varepsilon$ on relative humidity for samples 1.1 (*d*), 2.2 (*e*), 4.4 mm (*f*) with frequency variation from 200 Hz to 5 MHz

the higher the frequency, the lower the impedance $Z$, at the same time, at high frequencies, the sensitivity of the impedance $Z$ to changes in humidity decreases (Fig. 4).

We investigated the dependence of relative dielectric constant on humidity in the frequency range from 200 Hz to 5 MHz for three sample thicknesses (Fig. 4, *d*–*f*). As can be seen from Fig. 4, changing the thickness of $(CaSO_4 \cdot 2H_2O)_{0.95} - (CuSO_4 \cdot 5H_2O)_{0.05}$ samples has little effect on the behavior of the relative permittivity, i.e., the frequency dependence of the dielectric constant, and its dependence on increasing relative humidity (RH). All samples had the highest sensitivity at 200 Hz. With increasing frequency, the dielectric constant decreases for all investigated sample thicknesses and simultaneously the moisture sensitivity deteriorates.

We do not observe resonance dispersion arising from electron and ion polarization. In the case of resonance polarization, we should observe an increase in dielectric constant over a certain frequency range, but this does not happen. The dispersion of the relative permittivity $\varepsilon$, expressed as its monotonic decrease with increasing frequency, is called relaxation. This is characteristic of the dipole and interlayer mechanisms of polarization [20]. As can be seen from Fig. 4, with increasing frequency of electric current, the value of relative permittivity $\varepsilon$ decreases, and its dependence on relative humidity RH weakens. The relative permittivity $\varepsilon$ depends weakly on the sample thickness over the entire frequency range.

The expression used to determine the sensitivity of impedance humidity sensors is as follows

$$S_z = \frac{Z(40) - Z(RH)}{Z(40)} \cdot 100\%. \quad (1)$$

The effect of relative humidity RH on the sensitivity of impedance humidity sensors was measured by placing samples in a chamber with known temperature and relative humidity varying from 40 to 80%. The sensitivity of the $S_z$ impedance moisture sensors was investigated for samples with thicknesses of 1.1, 2.2, and 4.4 mm at current frequencies of 200 Hz and 5 MHz. The sensitivity of the sensor $(CaSO_4 \cdot 2H_2O)_{0.95} - (CuSO_4 \cdot 5H_2O)_{0.05}$, expressed as a percentage, decreased by a factor of 4 when the frequency was increased from 200 Hz to 5 MHz for all sample thicknesses. Increasing the AC frequency degrades the sensitivity of the impedance humidity sensor.

With increasing frequency, the value of impedance $Z$ decreased, and simultaneously the values of active and reactive components of resistance decreased. It can be suggested that our samples $(CaSO_4 \cdot 2H_2O)_{0.95} - (CuSO_4 \cdot 5H_2O)_{0.05}$ may exhibit interlayer polarization characteristic of inhomogeneous dielectrics containing impurities. In these dielectrics, free electrons and impurity ions move inside some structural inclusion, which is likened to a huge polarized molecule. This polarization is observed in a constant electric field or at low frequencies of the exciting electromagnetic field. Dipole polarization is typical of polar dielectrics. This mechanism may also contribute to the relative dielectric constant of our samples, given their ability to accumulate dipole water molecules and given the presence of boundary layers in the contact area. As can be seen from Fig. 4, the relative permittivity increases with increasing humidity at all frequencies and hence the capacitance of the sample $C$, which is a flat capacitor, is

$$C = \frac{\varepsilon \varepsilon_0 S}{d}, \quad (2)$$

where $S$ — the area of the plates of the capacitor, $\varepsilon$ — the relative permittivity of the sample material, $\varepsilon_0$ — the vacuum constant. The capacitance of the sample $C$ increases with increasing $\varepsilon$, hence, due to volume polarization, the reactive component $X$ of the complex impedance $Z$, which is capacitive in our case, should decrease with increasing humidity:

$$X = \frac{1}{C\omega}. \quad (3)$$

This is consistent with the decrease in complex impedance $Z$ with increasing humidity (Fig. 4).

Fig. 5 shows the results of impedance spectroscopy of $(CaSO_4 \cdot 0.5H_2O)_{0.95} - (CuSO_4 \cdot 5H_2O)_{0.05}$ samples of three thicknesses — 1.1, 2.2, and 4.4 mm in the relative humidity range of 30–80%.

Godographs obtained at high humidity (Fig. 5, *d–f*), representing an arc of varying degrees of closure, are often observed for homogeneous samples with low-resistance contacts [20]. We are dealing with a system with mixed conductivity. The similarity of impedance behavior in samples of different thicknesses at low humidity (Fig. 5, *a–c*) and similar dynamics of semicircular locus formation at high humidity suggest that the conductivity at high frequencies is due to the predominance of grain conductivity. These conclusions are confirmed including low complex resistivity $Z$over the entire moisture range at all sample thicknesses (Fig. 4). The drop in the value of $Z$ from low to high frequencies confirms the strong influence of the double interface layer in the contact area on the complex resistance. The dependence of the imaginary part $\mathrm{Im}(Z)$, due to capacitance, on the real part $\mathrm{Re}(Z)$ decreases with increasing moisture content for all sample thicknesses (Fig. 5).

For all sample thicknesses, a further increase in relative humidity (RH) leads to the formation of a locus half-circle (Fig. 5, *d–f*). A disordered dielectric that readily absorbs water from the air and readily gives it back until equilibrium is reached is a complex circuit. The analytical expression for the impedance of the circuit under consideration is cumbersome and difficult to analyze. The behavior of the impedance locus can be described qualitatively. We propose to use the traditional substitution scheme of a solid electrolyte cell with blocking electrodes without taking into account the grain boundary resistance (Fig. 6).

For high frequencies, due to the small value of the complex resistance compared to $R$, the effect of capacitance $C_2$ can be neglected. Consequently, the high-frequency part of the locus is a semicircle of radius $R/2$, passing through the origin. For low frequencies in the limit ($\omega \to 0$), conversely, we neglect the effect of capacitance $C_1$ (which corresponds to a very large impedance of $1/(\omega C_1)$). Such a scheme is used to describe electrochemical cells considering geometric capacitance. $R$ corresponds to the sample resistance, $C_2$ — the capacitance of the double interface layer, $C_1$ — the geometric cell capacitance (the capacitance of the sample enclosed between the electrodes).

To demonstrate the potential for practical application as an air humidity sensor, the response time and impedance reduction time were measured for $(CaSO_4 \cdot 2H_2O)_{0.95} - (CuSO_4 \cdot 5H_2O)_{0.05}$ samples of two thicknesses — 1.1 and 2.2 mm. The samples were placed

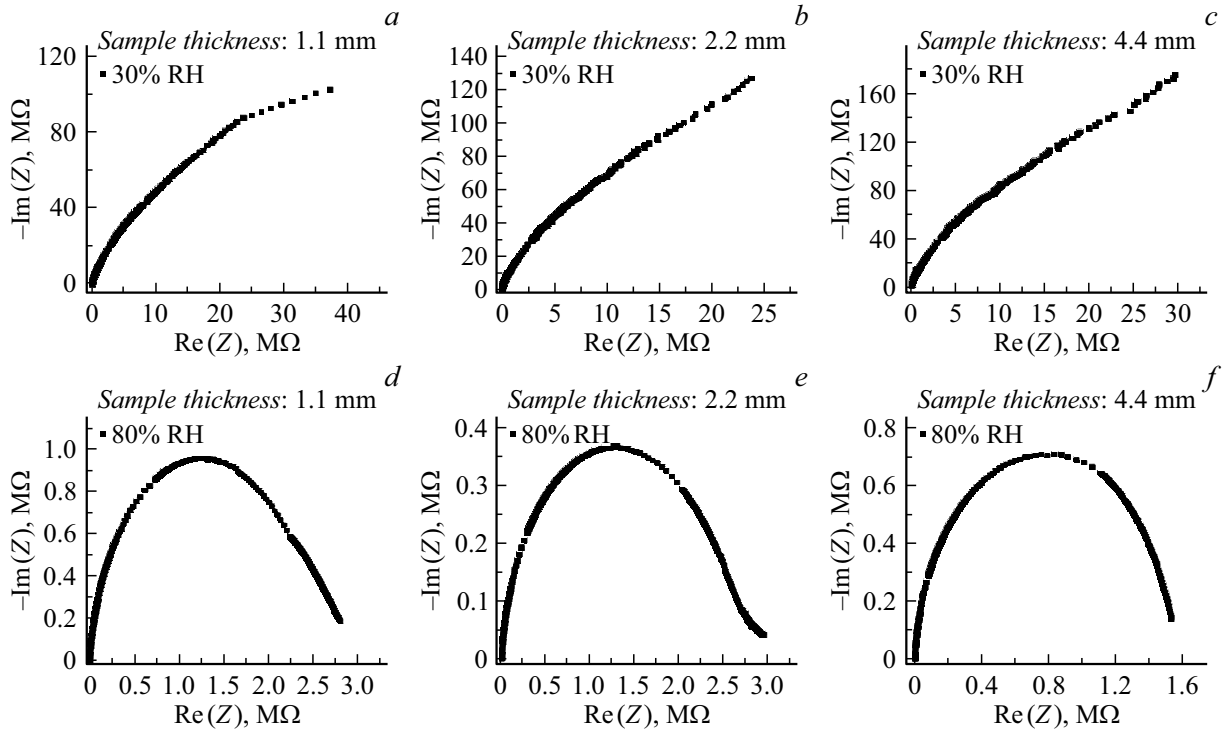


**Figure 5.** Impedance spectroscopy results of samples $(CaSO_4 \cdot 0.5H_2O)_{0.95} - (CuSO_4 \cdot 5H_2O)_{0.05}$ of three thicknesses — 1.1, 2.2 and 4.4 mm at a relative humidity range of 30 −80%.

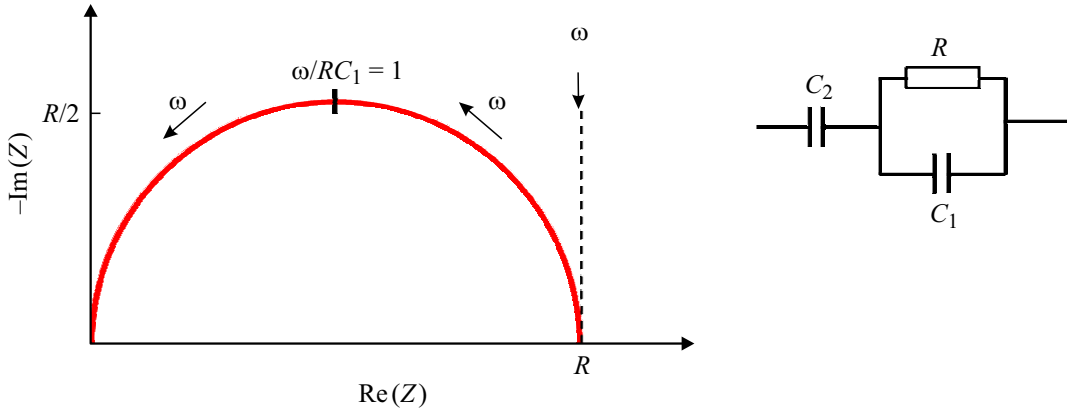


**Figure 6.** Equivalent scheme of a solid-electrolyte cell with blocking electrodes without taking into account grain boundary resistance

in a chamber with 90% relative humidity, resulting in an impedance decrease from 13 to 11 MΩ (Fig. 7, *a*) with a sample thickness of 1.1 mm. After removing the sample from the chamber to the environment (air temperature 28 °C, RH 30%), the impedance of the sample was restored. The response time was 5 s and the reduction time was 3 s for the 1.1 mm thick specimen; for the 2.2 mm thick specimen, these times were 7 and 5 s, respectively. After that, the cycle was repeated.. Thus, cycling of the composite-based sensor $(CaSO_4 \cdot 2H_2O)_{0.95} - (CuSO_4 \cdot 5H_2O)_{0.05}$ can be arranged without additional heating.

Fig. 7 shows the impedance switching cycles in the relative humidity range of 30−90%. The impedance curves quickly return to the original state after the humidity is turned off. Samples of all three thicknesses showed impedance variation at frequency 1 kHz and voltage 1 V, the impedance values for different thicknesses differed slightly. As can be seen from Fig. 4, at frequencies 200, 500 Hz and 1 kHz, the impedance of $Z$ had the maximum sensitivity to changes in relative humidity.

### 2.2. Composite samples: whiskers $CaSO_4 \cdot 2H_2O$ as reinforcing filler in epoxy matrix

Tensile and compression tests on samples of composite epoxy resins containing 0, 5, 10, and 15% of filamentary $CaSO_4 \cdot 2H_2O$ crystals were performed on an Instron 3369 universal testing machine. Fig. 8, *a* shows the dependence

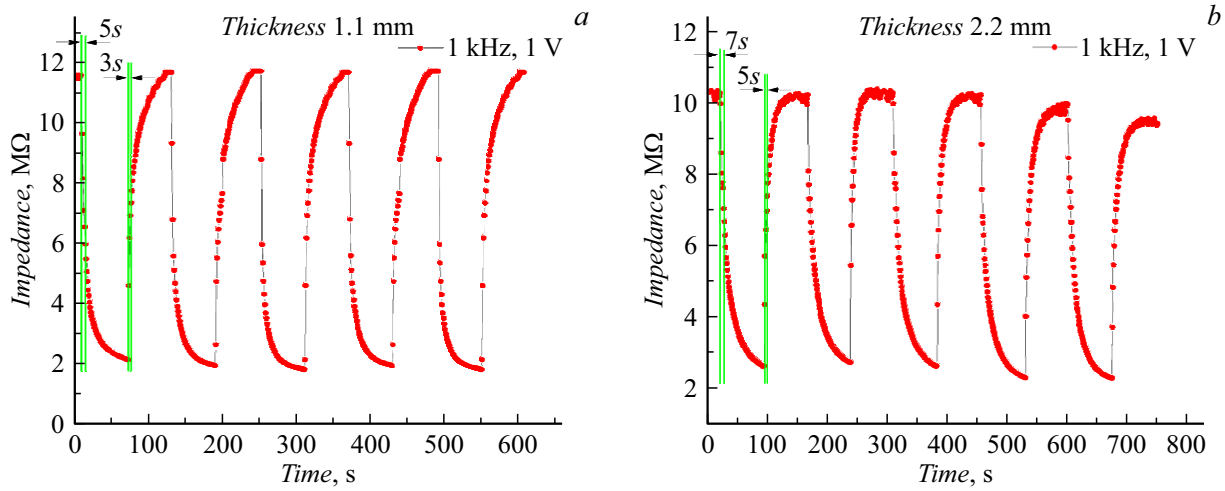


**Figure 7.** Impedance switching cycles over a relative humidity range of 30 −90% for samples $(CaSO_4 \cdot 2H_2O)_{0.95}-(CuSO_4 \cdot 5H_2O)_{0.05}$ thicknesses of 1.1 (*a*) and 2.2 mm (*b*).

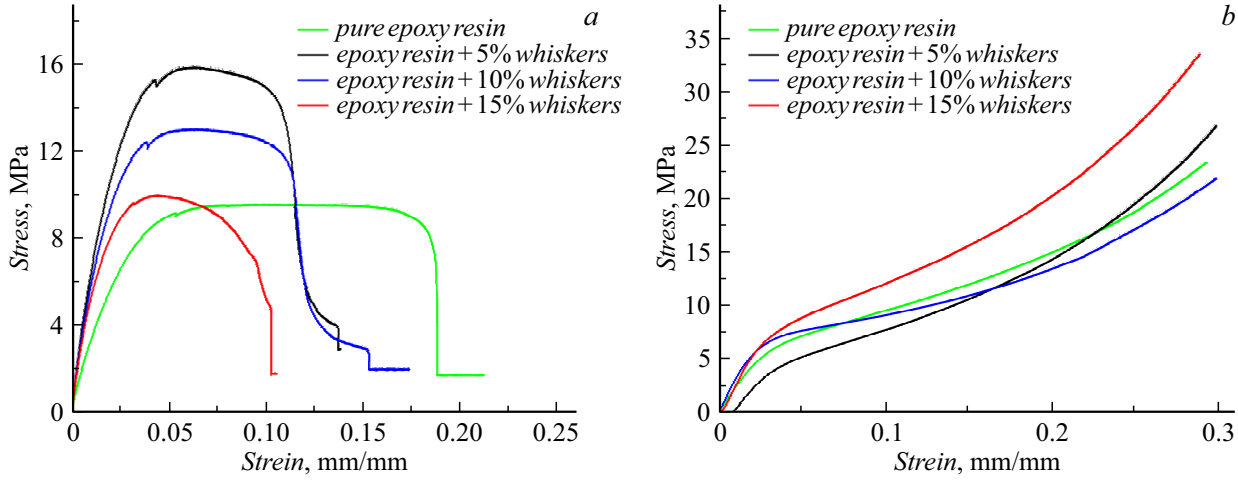


**Figure 8.** *a* — stress-strain diagram for samples of composite epoxy resin containing 0, 5, 10 and 15% of $CaSO_4 \cdot 2H_2O$ filamentary crystals, obtained in tension; *b* — the same in strain compression.

of tensile stress on strain. Samples with 5% whisker content showed an increase in total elasticity (increasing initial part of the curves), an increase in local yield stress and a decrease in the magnitude of the sample rupture strain compared to pure epoxy resin. In the initial parts of the curves corresponding to the elastic deformation (Fig. 8, *a*), its growth was observed for composites with 5% of whiskers, and then a decrease as the whisker concentration increased up to 15%. The elastic deformation of all composite formulations was found to be higher than that of pure epoxy resin.

As can be seen in Fig. 8, *a*, the sample containing 5% of filamentary $CaSO_4 \cdot 2H_2O$ crystals showed the highest tensile stress. Further increasing the whisker concentration to 15% resulted in a steady decrease in the tensile stress, although it still remained higher than that of pure epoxy. Fig. 8, *b* shows the compression test results of the composite specimens. It can be seen from the stress-strain relationship that only the sample with 15% whisker content shows a significant increase in compressive stress compared to pure epoxy resin.

## Conclusions

In result of the study of electrical conductivity, composite samples of citrogypsum $(CaSO_4 \cdot 2H_2O)$,doped with copper sulfate $(CuSO_4 \cdot 5H_2O)$, by impedance spectroscopy in the frequency range of 200 Hz−5 MHz at an AC signal amplitude of 1 V without DC polarization, the effect of environmental humidity on the value of the total complex resistance $Z$ and relative permittivity $\varepsilon$ was determined. Experimentally by impedance spectroscopy on $(CaSO_4 \cdot 2H_2O)_{0.95}-(CuSO_4 \cdot 5H_2O)_{0.05}$ samples, it is found that with increasing thickness of 1.1 mm → 2.2 mm → 4.4 mm the resistance of $Z$ in-

creases, e.g., at 40% humidity at 200 Hz, from 90 M $\Omega \rightarrow 130\,M\Omega \rightarrow 180\,M\Omega$, respectively.

At frequencies above 100 kHz, the sensitivity to changes in relative humidity was minimal for all sample thicknesses. For all thicknesses, the complex resistance decreases sharply in the frequency range from 200 Hz to 1 kHz with increasing relative humidity. As the frequency increases from 200 Hz to 5 MHz, the impedance of an $Z$ sample with a thickness of 1.1 mm decreases, for example, from 90 MΩ to 0.7 kΩ at a relative humidity of 40%. At high frequencies from 100 kHz to 5 MHz, the value of $Z$ is small and varies slightly with increasing moisture content for all sample thicknesses and decreases with increasing frequency. Thus, the higher the frequency, the lower the impedance $Z$, at the same time, at high frequencies, the sensitivity of the impedance $Z$ to changes in humidity decreases (Fig. 4),*a*–*c*). In the relative humidity range of 40 – 80% at a temperature of 28 °C, a relaxation dispersion of the relative permittivity is observed, expressed as a monotonic decrease in the relative permittivity $\varepsilon$ with increasing frequency (Fig. 4, *d*– *f*). It is assumed to be characteristic of dipole and interlayer polarization mechanisms.

Interlayer polarization is observed in inhomogeneous dielectrics containing impurities; such an inhomogeneous dielectric is our samples $(CaSO_4 \cdot 2H_2O)_{0.95}$–$(CuSO_4 \cdot 5H_2O)_{0.05}$ at low frequencies. In these dielectrics, free electrons and impurity ions move inside some structural inclusion, which is likened to a huge polarized molecule. Dipole polarization is typical of polar dielectrics. This mechanism may also contribute to the relative dielectric constant of our samples, given their ability to accumulate dipole water molecules and the presence of boundary layers near the metal contacts. Based on the observation of impedance locuses of $(CaSO_4 \cdot 2H_2O)_{0.95}$–$(CuSO_4 \cdot 5H_2O)_{0.05}$ samples at elevated humidity, an equivalent scheme of solid electrolyte cell with blocking electrodes without considering the grain boundary resistance is proposed. When the relative humidity was varied in the range of 30 –90%, the response and impedance reduction times for $(CaSO_4 \cdot 2H_2O)_{0.95}$–$(CuSO_4 \cdot 5H_2O)_{0.05}$ samples were measured without heating the samples. The response time was 5 s and the reduction time was 3 s for the 1.1 mm thick specimen; for the 2.2 mm thick specimen, these times were 7 and 5 s, respectively. The possibility of practical application of composite $(CaSO_4 \cdot 2H_2O)_{0.95}$–$(CuSO_4 \cdot 5H_2O)_{0.05}$, obtained on the basis of citrohypsum $(CaSO_4 \cdot 2H_2O)$, which is a waste product of the technological process of citric acid production, as a new material of air humidity sensor is shown.

The possibility of using $CaSO_4 \cdot 2H_2O$ whiskers to improve the mechanical properties of epoxy resin and obtain composite material is shown. In dependence on the percentage content of filamentary $CaSO_4 \cdot 2H_2O$ crystals in the epoxy resin, an improvement in the mechanical properties of the composite was found. The composite containing 5% $CaSO_4 \cdot 2H_2O$, whiskers showed the highest increase in tensile stresses, while the specimen with 15% whiskers showed the highest compressive strain resistance compared to pure epoxy resin specimens.

Depending on the practical application, increased tensile or compression characteristics may be important. Epoxy polymers make up a significant portion of fiber-filled composite matrices used in household, automotive, and aerospace applications [21]. A significant advantage of our composite is its low cost and environmental component, since the whiskers were obtained from citrogyps $CaSO_4 \cdot 2H_2O$, which is a waste product of industrial production of citric acid. In future, the process of producing an epoxy resin composite containing $CaSO_4 \cdot 2H_2O$ whiskers will be further investigated to optimize the material properties. In future, the process of producing an epoxy resin composite containing $CaSO_4 \cdot 2H_2O$ whiskers will be further investigated to optimize the material properties.

### Funding

The research was carried out within the framework of the state task for the creation of new laboratories in 2021 including under the guidance of young promising specialists of the national project „Science and Universities“, on the scientific theme „Development of scientific and technological foundations for the creation of a comprehensive technology for processing gypsum-containing waste from various industrial enterprises“, (FZWG-2021-0017).

### Conflict of interest

The authors declare that they have no conflict of interest.

## References

[1] X. Tao, Sh. Liao, Y. Wang. EcoMat., **3**, e12083 (2021). DOI: 10.1002/eom2.12083
[2] C. Magazzino, M. Mele, N. Schneider, S. Sarkodie. Sci. Total Environ., **755**, 142510 (2021). DOI: 10.1016/j.scitotenv.2020.142510
[3] K. Wang, X. Qian, L. Zhang, Y. Li, H. Liu. ACS Appl. Mater. Interfaces, **5** (12), 5825 (2013). DOI: 10.1021/am4014677
[4] E. Traversa. Sensors and Actuators B, **23** (2–3), 135 (1995). DOI: 10.1016/0925-4005(94)01268-m
[5] Y. Li, M.J. Yang. Sensors and Actuators B, **85** (1–2), 73 (2002). DOI: 10.1016/s0925-4005(02)00055-2
[6] B. Adhikari, S. Majumdar. Prog. Polym. Sci., **29** (7), 699 (2004). DOI: 10.1016/j.progpolymsci.2004.03.002
[7] T. Fei, J. Zhao, Zh. Hongran, T. Kai. Sensors and Actuators B: Chemical, **208**, 277 (2015). DOI: 10.1016/j.snb.2014.11.044
[8] U. Kang, K.D. Wise. IEEE Transactions on Electron Devices, **47** (4), 702 (2000). DOI: 10.1109/16.830983
[9] V. Prashanth, G. Boby. IEEE Transactions on Instrumentation and Measurement, **64** (4), 902 (2015). DOI: 10.1109/TIM.2014.2361552
[10] F. Hossein-Babaei, P. Shabani. Sensors and Actuators B: Chemical, **205**, 143 (2014). DOI: 10.1016/j.snb.2014.08.061
[11] V. Matko, D. Donlagic. IEEE Transactions on Instrumentation and Measurement, **45** (2), 561 (1996). DOI: 10.1109/19.492787

[12] R. Selyanchyn, Sh. Wakamatsu, K. Hayashi, S.-W. Lee. Sensors, **15** (8), 18834 (2015). DOI: 10.3390/s150818834
[13] D. Bridgeman, J. Corral, A. Quach, X. Xian, E. Forzani. Langmuir, **30** (35), 10785 (2014). DOI: 10.1021/la502593g
[14] N. Radouane, A. Maaroufi. *Fiber Inclusions-Based Epoxy Composites and Their Applications* (E-Book), In S.J.S. Chelladurai, R. Arthanari, M.R. Meera (editors). Epoxy-Based Composites (E-Book), 2022, p. 126, ISBN 978-1-80355-161-6. DOI: 10.5772/intechopen.104118
[15] H. Abdellaoui, M. Raji, R. Bouhfid, A. el kacem Qaiss. *Failure Analysis in Biocomposites, Fibre-Reinforced Composites and Hybrid Composites* (Elsevier Ltd., 2019), p. 29–49. DOI: 10.1016/b978-0-08-102293-1.00002-4
[16] T. Sirimahasal, Y. Kalhong, L. Simasatitkul, S. Pranee, S. Seeyangnok. Key Engineering Mater., **803**, 351 (2019). DOI: 10.4028/www.scientific.net/KEM.803.351
[17] N.I. Alfimova, S.Yu. Pirieva, M.Yu. Elistratkin, I.S. Nikulin, A.A. Titenko. IOP Conf. Ser.: Mater. Sci. Eng., **945**, 012057 (2020). DOI: 10.1088/1757-899X/945/1/012057
[18] T.B. Nikulicheva, I.S. Nikulin, E.A. Pilyuk, V.S. Voropaev, N.I. Alfimova, V.B. Nikulichev, M.Yu. Saenko. IOP Conf. Ser.: Earth Environ. Sci., **845**, 012152 (2021). DOI: 10.1088/1755-1315/845/1/012152
[19] R.J. Hand. Br. Ceram. Trans., **96** (3), 116 (1997). ISSN: 0967-9782
[20] E. Barsoukov, J.R. Macdonald (eds.). *Impedance Spectroscopy. : Theory, Experiment, and Applications* (John Wiley & Sons, Inc., 2018), DOI: 10.1002/9781119381860
[21] D. Rajak, D. Pagar, P. Menezes, E. Linul. Polymers, **11** (10), 1667 (2019). DOI: 10.3390/polym11101667

*Translated by Y.Deineka*